water

MDPI

Article

Projected Streamflow and Sediment Supply under Changing Climate to the Coast of the Kalu River Basin in Tropical Sri Lanka over the 21st Century

T.A.J.G. Sirisena [1,2,*], Shreedhar Maskey [1], Janaka Bamunawala [1,2,3], Erika Coppola [4] and Roshanka Ranasinghe [1,2,5]

1 IHE Delft Institute for Water Education, 2611 AX Delft, The Netherlands; s.maskey@un-ihe.org (S.M.); bamunawala@uom.lk (J.B.); r.ranasinghe@un-ihe.org (R.R.)
2 Department of Water Engineering and Management, Faculty of Engineering Technology, University of Twente, 7522 NB Enschede, The Netherlands
3 Department of Civil Engineering, Faculty of Engineering, University of Moratuwa, Moratuwa 10400, Sri Lanka
4 Earth System Physics Section, The Abdus Salam International Centre for Theoretical Physics (ICTP), 11, I-34151 Trieste, Italy; coppolae@ictp.it
5 Department of the Harbour, Coastal and Offshore Engineering, Deltares, 2600 MH Delft, The Netherlands
* Correspondence: j.g.s.thotapitiyaarachchillage@utwente.nl; Tel.: +31-617029706

Abstract: Tropical countries are already experiencing the adverse impacts of climate change. This study presents projections of climate change-driven variations in hydrology and sediment loads in the Kalu River Basin, Sri Lanka. Bias-corrected climate projections (i.e., precipitation and temperature) from three high resolution (25 km) regional climate models (viz., RegCM4-MIROC5, MPI-M-MPI-ESM-MR, and NCC-NORESM1-M) are used here to force a calibrated hydrological model to project streamflow and sediment loads for two future periods (mid-century: 2046–2065, and end of the century: 2081–2099) under two representative concentration pathways (i.e., RCPs 2.6 and 8.5). By the end of the century under RCP 8.5, all simulations (forced with the three RCMs) project increased annual streamflow (67–87%) and sediment loads (128–145%). In general, streamflow and sediment loads are projected to increase more during the southwest monsoon season (May–September) than in other periods. Furthermore, by the end of the century, all simulations under the RCP 8.5 project a shift of streamflow and sediment loads in the southwest monsoon peak from May to June, while preserving the peak in the inter-monsoon 2 (in October). The projected changes in annual sediment loads are greater than the projected changes in annual streamflow (in percentage) for both future periods.

Keywords: Kalu river basin; regional climate models; streamflow; sediment loads

Citation: Sirisena, T.A.J.G.; Maskey, S.; Bamunawala, J.; Coppola, E.; Ranasinghe, R. Projected Streamflow and Sediment Supply under Changing Climate to the Coast of the Kalu River Basin in Tropical Sri Lanka over the 21st Century. *Water* **2021**, *13*, 3031. https://doi.org/10.3390/w13213031

Academic Editor: Peng Gao

Received: 10 September 2021
Accepted: 25 October 2021
Published: 28 October 2021

1. Introduction

The impact of climate change on natural and man-fabricated systems has been observed on all landmasses and oceans in the last few decades [1]. It has been observed that after 1990, mean land surface air temperature has increased by more than 0.5 °C compared with global mean surface temperature. Furthermore, this warming has affected increases in high-intensity precipitation events and extreme weather events globally (e.g., heatwaves) [2]. Projections indicate that the global mean surface temperature is likely to increase by 0.3–4.8 °C by the end of the 21st century (2081–2100) (relative to 1986–2005). However, changes in precipitation are expected to vary highly across the world [3]. More intense and frequent extreme precipitation events are anticipated in mid-latitudes and the wet tropics, predominantly due to increased surface temperature [3].

According to the Climate Risk Index (CRI) analysis [4], Sri Lanka was among the ten countries in the world that was most affected by climate change in 2018. Sri Lanka is expected to be significantly affected by increases in surface temperature [5], changes

in precipitation variability (both spatial and temporal distribution), increases in extreme climatic events causing floods, landslides, and droughts, and sea-level rise [6]. Evidence suggests that the country's climate has already changed over the past few decades [5,7,8]. For example, a decrease in average annual rainfall of Sri Lanka by 144 mm was estimated during the 1961–1990 period compared with 1931–1960 (Chandrapala, 1996 [9] cited in Eriyagama et al., 2010 [8]). The same study also indicates that the mean annual temperature in Sri Lanka has increased at a rate of 0.48 °C over the 1961–1990 period.

Despite being the second largest river basin in Sri Lanka, the Kalu River Basin (KRB, 2787 km^2) annually drains (4000 million m^3) more water than the largest river basin (Mahaweli River Basin, 10,488 km^2) into the Indian Ocean [10]. Unlike the Mahaweli River, which is heavily regulated, the Kalu river is still in pristine condition with no major flow regulations along its mainstream and major tributaries. The KRB (Figure 1) is important to the Sri Lankan economy because of agricultural production, and the high population density in the basin. Unfortunately, the basin's middle and lower flood-plain areas experience frequent floods during the southwest monsoon (May to October) with negative socio-economic impacts [10–12]. These conditions may vary under projected climate change, and hence a proper assessment of basin-scale impacts is vital to manage water resources and reduce flood hazards in the basin.

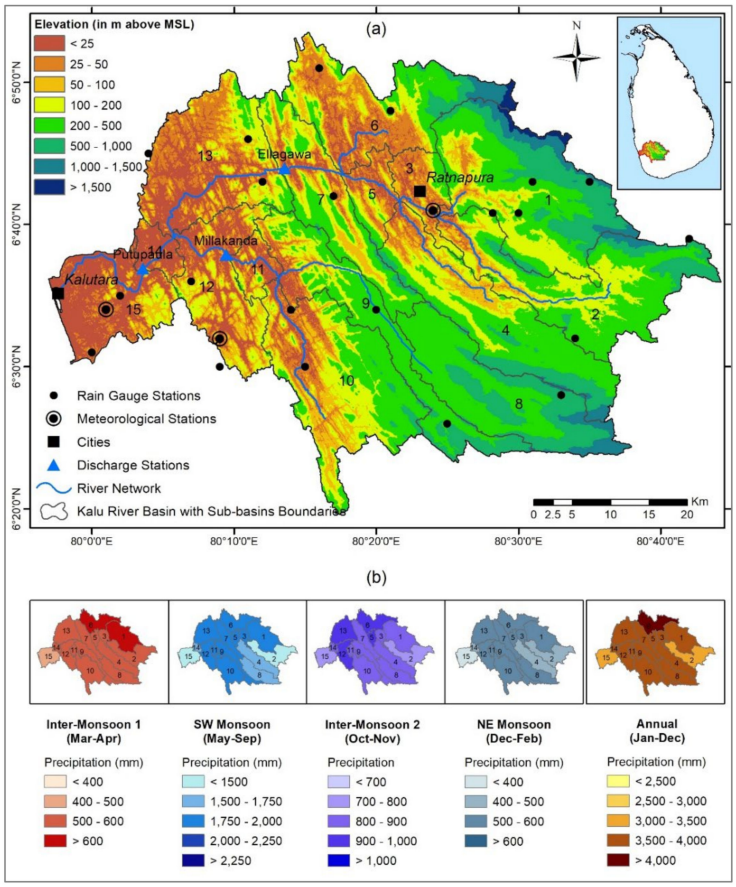

Figure 1. Kalu River Basin, Sri Lanka (**a**) and spatial distribution of seasonal and annual variations in precipitation over the basin for the period of 1990–2015 (**b**). MSL: mean sea level, SW: southwest, and NE: northeast. Precipitation of each of the sub-basins was obtained from interpolated gauge data (more details in Section 2.1).

Climate change projections from general circulation models (GCMs) are typically used in forcing hydrological models to simulate the impacts at river basins. However, for a small river basin such as the Kalu, the spatial resolution of GCM data (i.e., precipitation, and temperature at 1.25–3 °C resolution) is coarse to accurately represent the local hydro-

logical variabilities [13–16]. To address this issue, climate projection data are downscaled (with dynamic or statistical techniques) before being used in hydrological models for small basins. Generally, dynamic downscaling is preferred, which is based on running a regional climate model (RCM, with a spatial resolution of 25–50 km) forced with GCM outputs, together with relevant regional information (e.g., orography and land-use) [15]. However, RCM outputs may need further correction for bias for river basins with high hydrological variability.

Only a few studies have investigated future climate (i.e., precipitation and temperature) and hydrological responses in the KRB (e.g., Nyunt et al. (2012) [17] and Schulz and Kingston (2017) [18]). To the best of our knowledge, to date, no studies have used high-resolution (25 km) regional climate models (RCMs) data to project future streamflow and sediment loads at the basin level in any major river basins in Sri Lanka. This study is the first to use the RCM outputs of the latest greenhouse gas (GHG) emission scenarios (RCPs) to project streamflow and sediment loads of the KRB. Here, we used three RCMs under the two end-member IPCC AR5 scenarios: RCP 2.6 and RCP 8.5.

2. Materials and Methods

2.1. Data Used in This Study

The Kalu River originates in the Samanala mountain range in south-central Sri Lanka and garners rainfall on the western slopes, and discharges into the sea at Kaluthara after traversing approximately 129 km (Figure 1a). The Kalu River has steep gradients until Rathnapura (Figure 1a) and a very mild gradient in the lower part. The soil water assessment tool (SWAT) ([19,20], ArcSWAT 10.5 version), a catchment hydrological model, was used to simulate the hydrological responses of the basin. It requires various geo-spatial data (i.e., topography, land-use, and soil type). A 90 × 90 m^2 resolution digital elevation map (DEM) from the Shuttle Radar Topography Mission (SRTM, accessed in 1st August 2016) [21] was used to delineate the basin (Figure 1). Land-use data with 300 × 300 m^2 resolution were obtained from the Survey Department of Sri Lanka. Much of the basin's land area is utilized for rain-fed agriculture with paddy rice (8.5%), rubber (27%), tea (6.5%), and other crops (i.e., cinnamon, coconut, 19.4%), scattered throughout the basin. The forest cover is 19% of the total basin area. A soil map at 7 × 7 km^2 resolution was obtained from the Food and Agriculture Organization [22]. Clay-rich Acrisol is the most prominent (~98% of basin area) soil type in the basin.

Meteorological data were obtained from two institutions: the Department of Meteorology and Lanka Hydraulic Institute, Sri Lanka. Daily precipitation data were obtained from 25 rain gauge stations (Figure 1) for the 1990 to 2015 period. These data were interpolated over a 5 × 5 km^2 grid and averaged over each sub-basin for use in the model using the inverse distance elevation weighted (IDEW) method. This interpolation and averaging over sub-basin were carried out using the Hykit tool [23]. Sri Lanka's hydrological year is divided into four main seasons based on monsoon rainfall: inter-monsoon 1 (IM-1; March to April), southwest monsoon (SWM; May to September), inter-monsoon 2 (IM-2; October to November), and northeast monsoon (NEM; December to February) [11]. The highest rainfall is received during the SWM period (Figure 1b). Since the Kalu River Basin is located in the country's southwest monsoon belt, some parts of the basin receive more than 2000 mm of rainfall between May and September. The average annual rainfall in the Kalu basin is approximately 3800 mm, and its average annual runoff is ~5550 million m^3 (at Putupaula station, Figure 1a). The observed daily temperature (minimum and maximum) data at three meteorological stations (Figure 1a) over the 1990–2015 period were used in the hydrological model. The average daily temperature in the basin is ~25 °C.

Daily streamflow data (collected from the Department of Irrigation, Sri Lanka) are available for three gauging locations (Ellagawa, Millakanda, and Putupaula, Figure 1a) for the 1991–2015 period. However, streamflow data from the Ellagawa and Putupaula gauging stations are unreliable after 2000 due to errors in the respective rating curves. For this reason, only the streamflow data from 1990 to 2000 were used to calibrate the model.

2.2. Hydrological Model (SWAT) Setup and Calibration

SWAT is a comprehensive (semi-) distributed model with sub-basins and hydrological response units (HRUs). The Kalu River Basin was divided into 15 sub-basins based on the threshold of stream definition and discharge gauging stations (Figure 1). The sub-basins were further divided into a total of 161 HRUs. HRUs are based on defined thresholds of land-use, soil, and slope categories [20,24].

For hydrological process simulation, the following methods are used: the Hargreaves method for potential evapotranspiration (PET), soil conservation services–curve number (SCS-CN) method for surface runoff volume and infiltration volume, and variable storage method for river flow routing. For soil erosion simulation from HRUs, SWAT uses the modified universal soil loss equation (MUSLE).The model considers deposition and degradation processes for sediment transport in the river reaches and uses the Bagnold's equation to determine the maximum sediment volume transported through a channel during the sediment routing [20]. All other processes are based on the SWAT default setting.

The model was calibrated for the streamflow and sediment loads at different gauging stations and the basin outlet. Model parameters and their initial ranges were selected following suggestions made in past studies [25–27]. Initial ranges of the chosen parameters are presented in Table S1 of Supplementary Materials. The calibration parameters represent the land cover, topographic conditions, soil properties, and groundwater process of the basin. Streamflow of the basin was calibrated prior to sediment loads. Other parameters were set as default values.

In the calibration run, the first year of simulations (1990) was used as the warm-up period. The Sequential Uncertainty Fitting algorithm version 2 (SUFI-2) [28] in the SWAT-Calibration and Uncertainty Program (SWAT-CUP) [25] was used for automatic model calibration and validation because several successful studies have used SUFI-2 for this purpose [29–31]. The Modified Nash–Sutcliffe efficiency (MNSE) [25], which has been proven to perform better than NSE, particularly in low flow regimes [32,33], was used as the objective function. Several iterations (each with 500 simulations) were carried out for calibration. At every iteration, the SUFI-2 suggests a new parameter range for the next iteration. However, parameter ranges for the subsequent iteration were selected by considering the ranges suggested by the calibration program (i.e., SUFI-2) and parameters' physically allowable upper and lower limits. The iteration process was terminated when the improvement in the objective function between two successive iterations was insignificant. Once a gauging station was calibrated, the optimized model parameters were fixed for all the sub-basins draining to that gauging station, and the calibration was continued to the next downstream station. This procedure was repeated for each discharge gauging station starting from the farthest upstream station (Ellagawa), tributary (Millakanda), and to the final downstream station (Putupaula) (Figure 1a).

Regrettably, the available sediment load observations (time series data) were insufficient to calibrate the model comprehensively for fluvial sediment loads. The manual soft calibration approach was used to adjust the model parameters related to the soil erosion and transport (Table S1) to obtain a reasonably calibrated model for the 1991–2000 period based on a few yearly sediment values: 0.768, 0.768, 0.672, and 0.576 million tons in 1976, 1984, 1991, and 2001, respectively [34].

Although only MNSE was used as the objective function, calibrated results were also assessed using other standard efficiency criteria such as Nash–Sutcliffe efficiency (NSE), percentage of bias (PBIAS), and coefficient of determination (R^2) [35].

2.3. Climate Projections and Bias Correction

Climatic data (i.e., precipitation and minimum and maximum temperatures) for KRB were obtained from three regional climate models (RCMs) simulations of the RegCM4 model [36] (details in Table 1). RCM data are particularly important for Sri Lanka because coarser-resolution general circulation model (GCM) data are found inadequate to capture the monsoon precipitation signal. These RegCM4 simulations are driven by three different

global climate models (GCMs) from the CMIP5 ensemble, selected based on their ability to represent the large-scale climatic features of the South Asian region [36]. This GCMs selection is also based on the climate sensitivity range of the CMIP5 ensemble models, such that one model was selected with low climate sensitivity, one with medium climate sensitivity, and one with high climate sensitivity [37].

Table 1. Regional climate model (RCM) predictions and observations over the basin for the 1991–2005 period. * based on 24 stations and ** based on 3 stations.

RegCM4 RCMs	Resolution	Average Annual Precipitation (mm)	Average of Daily TEMPERATURE (°C)	
			Minimum	Maximum
MIROC5	25 × 25 km^2	7090	22.4	26.4
MPI-M-MPI-ESM-MR	25 × 25 km^2	6630	22.4	26.6
NCC-NORESM1-M	25 × 25 km^2	4490	21.9	26.9
Observed		3800 *	22.7 **	31.5 **

During the baseline period (1991–2005), the RCMs produced significantly higher annual precipitation than what was estimated based on the observed rain gauges in the basin (3800 mm for 1991–2005) (Table 1). All three RCMs have roughly similar daily maximum and minimum temperatures for the baseline period (1991–2005, Figure S1), all of them underestimating the maximum daily temperature over the entire basin. For example, observation temperature estimates show that the maximum daily temperature is 31.5 °C during the baseline period, while the estimates from RCMs are 26–27 °C. Except for the 2 °C bias (underestimation by RCMs) in the northern part of the basin, RCMs model the daily minimum temperatures relatively close to the observed temperatures (Figure S1).

RCM data (i.e., precipitation, and maximum and minimum temperatures) were bias-corrected using the mean-bias correction method [38–40] at monthly steps. The calibrated SWAT model was forced with bias-corrected climate data to simulate streamflow and sediment loads. The analysis was carried out for two future periods: mid-century (2046–2065) and end-century (2081–2100), under two RCPs (i.e., RCP 2.6 and RCP 8.5). The projected changes in streamflow and sediment loads were compared with the model simulations forced with RCMs data for the baseline period (1991–2005).

3. Results and Discussion

3.1. Calibration of the Hydrological Model Using Observed Data (1991–2000)

Model calibration simulations produced 'very good' results at Ellagawa and Putupaula gauging stations, which are located in the main river (Figure 2) (see Moriasi et al. (2007) [35] for model evaluation criteria). However, at Putupaula, the low flows were underestimated. In addition, the model underestimated the streamflow at Millakanda. This underestimation is likely due to inadequate rainfall input, particularly in sub-basins 4, 8, and 9 (Figure 1) because the rain gauge stations are unevenly distributed in the Millakanda drainage area.

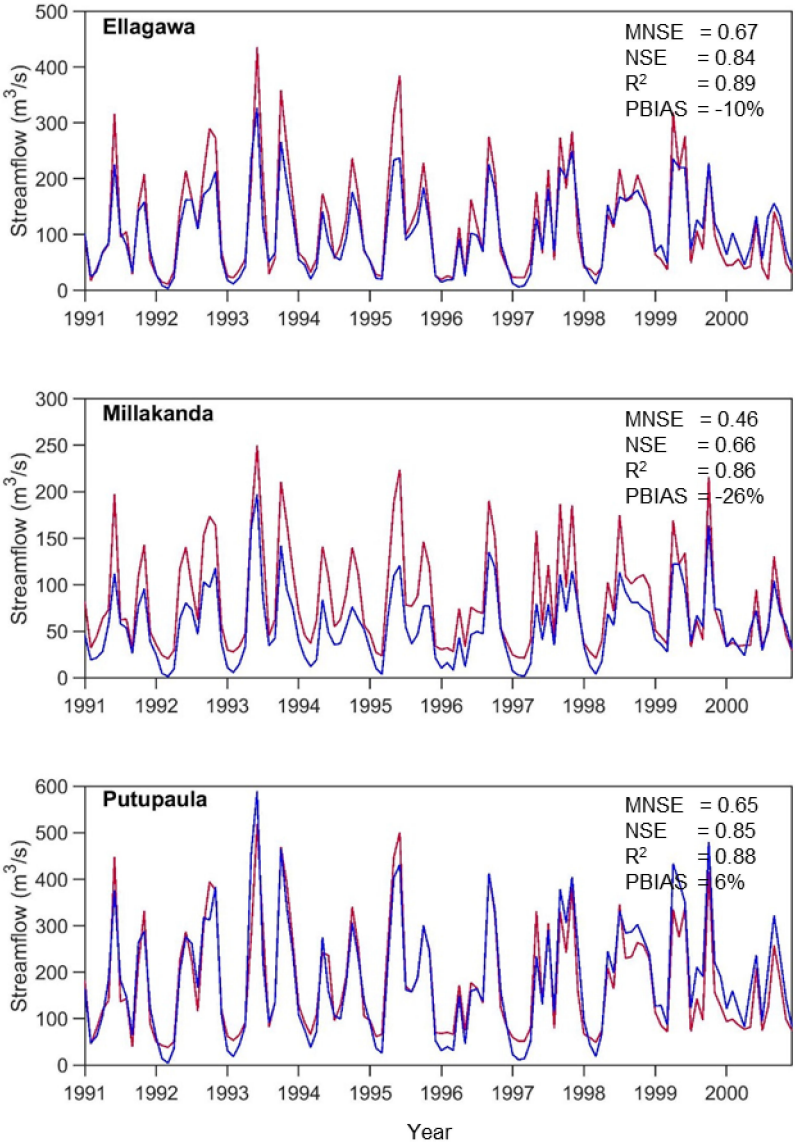

Figure 2. Comparison of simulated and observed monthly streamflow of the best simulations at three stations during the calibration period (1991–2000). Red and blue lines indicate the observed and simulated data, respectively.

In terms of sediment loads, the modeled sediment loads are about the same as the "observed" from different years. The average annual sediment load at the Kalu river outlet is estimated as $0.78 \pm 0.19 \times 10^6$ t/yr, whereas the average value of four-year observations is $0.70 \pm 0.09 \times 10^6$ t/yr. During 1976–2001, the annual average sediment load at the basin outlet is 70 t/ha/yr [34].

The simulated average sediment yield over the calibration period (1991–2000) ranged between 39 and 80 t/ha/yr (Figure 3a), with a basin-averaged value of 59 t/ha/yr. The highest soil loss is in sub-basins 6, 7, and 11, where rubber and tea are the dominant crops. The estimated mean yield did not vary significantly over the simulation period (Figure 3b). These results are in reasonable agreement with previous studies in Sri Lanka (e.g., Dissanayake and Rupasinghe (1996) [41] and Hewawasam (2010)) [42].

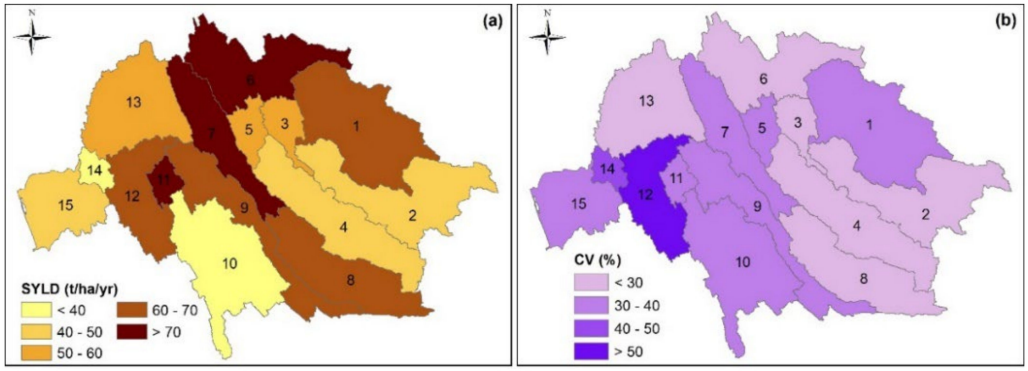

Figure 3. The model simulated (**a**) average annual sediment yield, and (**b**) coefficient of variation in sediment yield at sub-basin level for the baseline period (1991–2000) in Kalu River Basin.

3.2. Model Simulations for the Baseline Period Using Bias-Corrected RCMs Data

3.2.1. Streamflow

The simulations forced with bias-corrected RCM data (obtained from MIROC5, MPI-ESM-MR, and NCC-NORESM1-M) estimate the streamflow reasonably well. Table 2 compares the mean and standard deviations of simulated and observed monthly and annual streamflow at the most downstream station of the basin: Putupaula (located near the basin's outlet, Figure 1). The analysis is limited to 1991–2000 due to unreliable streamflow data after 2000 (see Section 2.2). In general, the simulation with NorESM1-M data outperforms the other two RCMs with some exceptions in the low flow period (January–March). The simulations with three RCMs performed well in the second high flow season (in October) with ±10% of the observed flow. Mean annual flows are re-produced (±10% of observed flow) by simulations forced with the three RCMs. However, all three RCMs underestimate low flows (during January–March, more than 20% of observed flow) with some exceptions in the results of the NorESM simulations. A possible reason for this underestimation is the fact that the calibrated model (driven by observed climate data) underestimates low flows in a few years of the study period (Figure 2). Furthermore, all RCMs reproduce the median and high flows quite accurately (mostly within ±10% of observed values), though they slightly underestimate high flows during August–October.

3.2.2. Sediment Loads

The mean annual sediment loads obtained from the simulations with calibrated parameters show reasonable agreement with the observations (within ± 10% of observations, Table 3). However, these results underestimate both SWAT simulations (forced with observed climate data, $0.78 \pm 0.19 \times 10^6$ t/yr (for 1991–2000)), and observed data ($0.70 \pm 0.09 \times 10^6$ t/yr, an average of four annual observations: 1976, 1984, 1991 and 2001) at the basin outlet, respectively. The standard deviations of 15 years of simulated sediment loads of each RCM exceed ±20% of the standard deviation of the observations. However, the standard deviation of the four observations is not statistically well-represented. Further, two years (1991 and 2001) are presented to compare the yearly observed and simulated values,. Except for underestimating sediment loads from MIROC5 for 1991 and NorESM for 2001, all other simulations overestimate the yearly sediment values, beyond 20% of observed values.

Table 2. Comparison of observed and simulated hydrological indices (mean and standard deviation (within bracket) based on monthly average streamflow) at Putupaula Gauging station (located near to the Kalu Basin Outlet) for 1991–2000. "Green, yellow, and red" represent the simulated streamflow value within ±10%, within ±20%, and beyond ±20% of observed streamflow, respectively.

Description	Observed (m^3/s)	Simulated (Driven by RegCM4 Data, m^3/s)		
		MIROC5	MPI-ESM	NorESM
Mean monthly flow				
January	92 (41)	60 (24)	67 (20)	81 (31)
February	66 (20)	45 (19)	43 (23)	54 (36)
March	64 (14)	42 (15)	44 (17)	61 (45)
April	137 (93)	121 (32)	98 (64)	156 (168)
May	231 (114)	183 (55)	226 (203)	293 (89)
June	301 (144)	199 (78)	212 (108)	258 (56)
July	188 (99)	169 (65)	174 (51)	205 (93)
August	134 (42)	121 (44)	123 (33)	135 (54)
September	218 (113)	203 (73)	185 (23)	200 (77)
October	315 (92)	314 (94)	296 (100)	298 (178)
November	262 (109)	293 (103	252 (87)	250 (102)
December	132 (67)	143 (68)	156 (54)	148 (28)
Mean annual flow	178 (29)	158 (22)	157 (36)	179 (38)

Table 3. Comparison of observed and simulated annual sediment loads at Kalu River Basin outlet for 1991–2005. "Green, and red" represent the simulated streamflow value within ±10%, and beyond ±20% of observed streamflow, respectively. * Observed data are available only for four years (1976, 1984, 1991, and 2001).

Description	Observed * (Million tons/yr)	Simulated (Driven by RegCM4, Million tons/yr)		
		MIROC5	MPI-ESM	NorESM
Mean	0.696	0.634	0.657	0.642
Standard deviation	0.092	0.198	0.265	0.194
Year 1991	0.672	0.594	0.918	1.084
Year 2001	0.576	0.846	0.742	0.487

3.3. Future Projections of Climate and Hydrology Using Bias-Corrected RCM Data under RCP 2.6 and 8.5

3.3.1. Changes in Future Climate

Precipitation

The RCPs data showed that the southwest (SW) monsoon and inter-monsoon would continue to bring high amounts of precipitation in the KRB. The basin is projected to experience significantly increased monsoon precipitation (May to September) for RCP 8.5 by the end of the century (Figure S2). Except for RegCM4/MIROC5, all the RCMs preserve the two peaks (in May and October) for RCP 2.6. RegCM4/MIROC5 projects a shift in peak precipitation from May to June at the end of the century. Under RCP 8.5, all RCMs project a shift in the SW monsoon peak from May to June by the end of the century, while RegCM4/MIROC5 also projects this shift during mid-century. RCMs under RCP 8.5 project the maximum variation in monthly precipitation (34–1038 mm) during the SW monsoon (May to September) at the end of the century, whereas RCMs under

RCP 2.6 project the minimum variation (−56 to 80 mm) at mid-century. Similarly, the maximum (23–282 mm during the end of the century) and minimum (−24 to 58 mm during mid-century) variations in precipitations are projected for RCP 8.5 and 2.6, respectively.

All models show an increase in average annual precipitation over the basin except RegCM4/MPI-ESM-MR which shows a decrease in the most downstream part of the basin (sub-basins 14 and 15) compared with the baseline period (Figure 4). The lowest increases in precipitation are projected in the eastern parts of the basin and the highest in the coastal areas. At the end of the century, the mean annual precipitation in the basin is projected to increase by 6–10% and 39–52% (compared with the 1991–2005 baseline period) for RCP 2.6 and RCP 8.5, respectively.

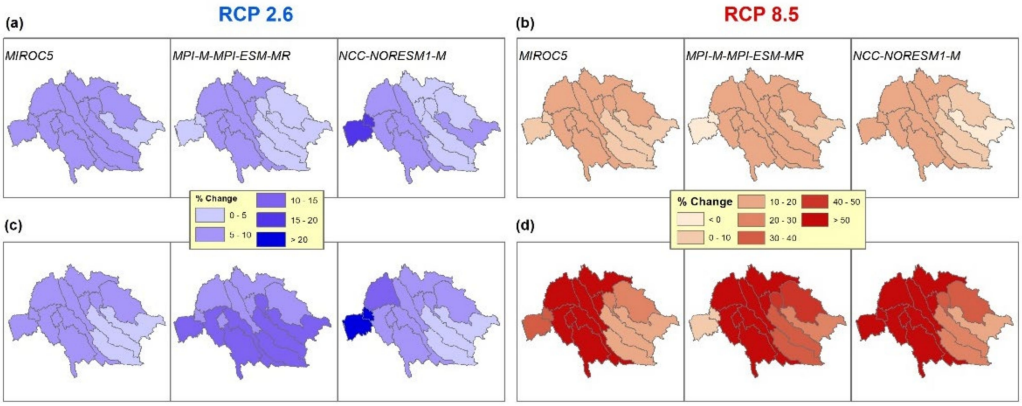

Figure 4. Percentage change in precipitation under RCP 2.6 (**left**) and RCP 8.5 (**right**) of three RegCM4 RCMs (from left to right MIROC5, MPI-M-MPI-ESM-MR, and NCC-NORESM1-M) compared with the baseline period (1991–2005) over each sub-basin of the Kalu River Basin. Two future periods are presented for each plot: 2046–2065 (**a**,**b**) and 2081–2099 (**c**,**d**).

RegCM4 RCM simulations also show an increase in annual precipitation over Sri Lanka by the 2080s of 39.6%, 35.5%, and 31.3% under A2, A1B, and B1 scenarios, respectively (compared with the baseline period, 1970–2000) [43]. Another study projected that the annual rainfall for 2006–2095, obtained from three downscaled GCMs (using quantile mapping correction), is likely to change by −0.5%–44% compared with 1971–2000 over the Mahaweli River Basin, Sri Lanka [44]. The annual precipitation over Sri Lanka is projected to increase by 11% (median from 42 downscaled GCMs using change factor method and quantile mapping) for 2046–2070 compared with 1976–2005 under RCP 8.5 [45]. The projected changes in mean annual precipitation of KRB found in our study appear to be higher than that projected for adjacent basins and Sri Lanka as a whole.

Temperature

All the selected models project an increase in the average daily maximum and minimum temperatures. However, the minimum temperatures are projected to increase more than the maximum ones (Figure 5). For both future periods, the temperature would increase approximately three times more under RCP 8.5 than under RCP 2.6. By the end of the century (2081–2099), the maximum temperature is projected to rise by 2.8–3.2 °C and the minimum by 3–3.2 °C for RCP 8.5 compared with the baseline period (Figure 5). Similar to these findings, Zheng et al. (2018) [45] found a 2 °C projected increase in temperature in Sri Lanka during 2046–2070 for RCP 8.5, which is the median value of 42 downscaled GCMs data.

3.3.2. Changes in Hydrology

All changes in streamflow and sediment loads for mid-century (2046–2065) and end of the century (2081–2099) periods were computed relative to the baseline period (1991–2005) (Section 3.2).

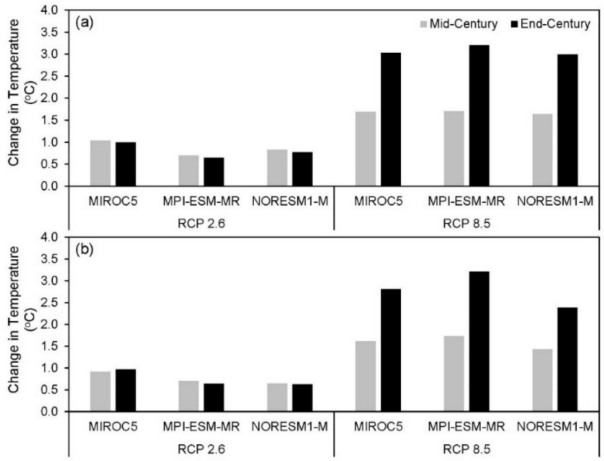

Figure 5. Changes of daily minimum (**a**) and maximum (**b**) temperatures in the Kalu River Basin under RCP 2.6 and RCP 8.5 of three RegCM4 RCMs compared with the baseline period (1991–2005) over the Kalu River Basin.

Streamflow

Simulations under RCP 8.5 project higher relative changes in the mean monthly streamflows than RCP 2.6, but neither one shows a clear pattern of increase or decrease over the year (Figure 6). The simulations forced with three RCMs show that the mean monthly streamflow at the basin outlet is projected to change between −26% and 71% under RCP 2.6 and between −47% and 76% under RCP 8.5 at mid-century. Similarly, monthly streamflows are expected to vary between −9% and 68%by the end of the century and −44% to 452% under RCP 2.6 and RCP 8.5, respectively. Simulations forced with RegCM4/NORESM1-M and RegCM4/MPI-ESM-MR show the highest increase (71% in February (NEM)) and decrease (−26% in March (IM-2)) under RCP 2.6 at mid-century. In contrast, under RCP 8.5, the highest changes in monthly streamflow would occur in June (during SWM, 452%) and March (during IM-1, −44%) at the end of the century, for the simulation forced with RegCM4/MPI-ESM-MR. This projected increase in streamflow in June coincides with the precipitation increase in the same month (Figure S2). In most cases (under two RCPs and two periods), simulations forced with RegCM4/MPI-ESM-MR are projected to decrease the streamflow during the inter-monsoon 1 (March–April). In general, streamflow is projected to increase more during the SWM period (May–October) than the other three seasons (Figure 6).

All simulations project the second peak of streamflow in October under both RCPs, which is in line with the baseline period observed data. Simulations forced with RegCM4/MIROC5 show a shift in the first peak flow month from May to June under both RCPs. The other two RCMs (RegCM4/MPI-ESM-MR and RegCM4/NORESM1-M) show mixed results for the shift in the peak flow month. For example, both RCMs have a projected peak in June at the end of the century for RCP 8.5. However, RegCM4/MPI-ESM-MR shows a peak in June, and other RCMs show a peak in May at the end of the century for RCP 2.6.

The mean annual streamflow is projected to increase in both future periods under both RCPs (Figure 7). Projections show an increase of 5–13% at mid-century and 9–20% at the end of the century for RCP 2.6, whereas an increase by 14–22% and 67–87% for RCP 8.5 during two periods, respectively. The projected variations in annual streamflows are always higher for RCP 8.5 than RCP 2.6. Zheng et al. (2018) [45] showed that the mean annual runoff of Sri Lanka is projected to increase by 31% (median value of hydrological simulations forced with downscaled 17 GCM projections using quantile mapping) for RCP 8.5 during 2046–2075 (relative to 1976–2005).

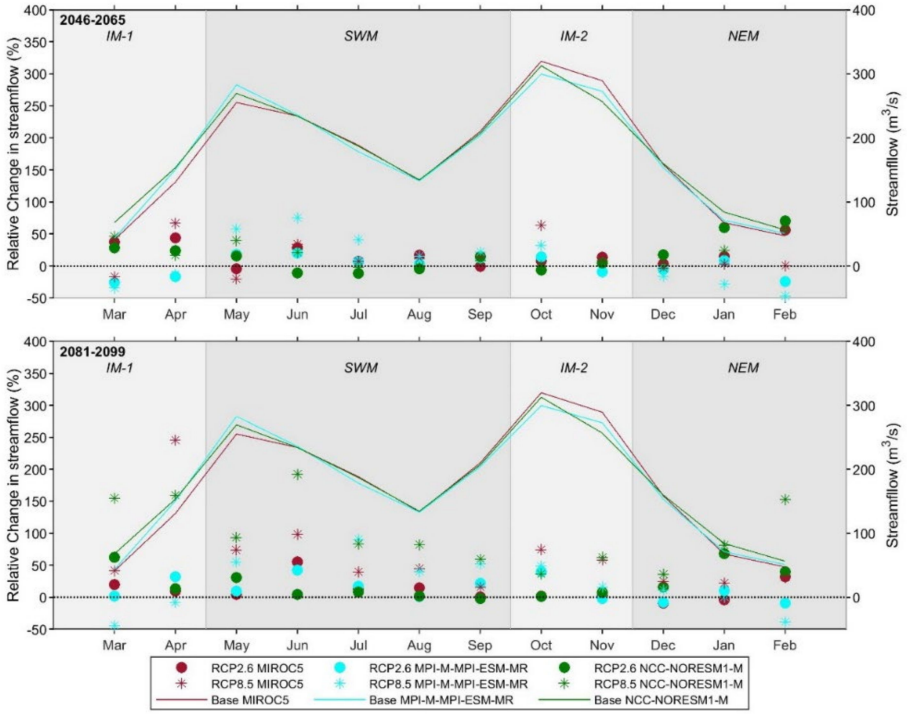

Figure 6. Percentage change in projected mean monthly streamflow at the basin outlet relative to the baseline period (1991–2005) and absolute values for baseline period for simulations forced with the three RegCM4 RCM data. In each panel, relative changes for future periods are in the primary (left Y-axis) and streamflow for baseline periods are in the secondary axis (right Y-axis). The top panel shows the mid-century period (2046–2065) and the bottom panel shows the end-century period (2081–2099). Each panel shows the results of simulations forced with three RegCM4 RCMs (MIROC5, MPI-M-MPI-ESM-MR, and NCC-NORESM1-M) under both RCP 2.6 (filled circles) and RCP 8.5 (asterisks). Shaded areas represent the four monsoon seasons.

Sediment loads

The projected relative change in fluvial suspended sediment loads is greater than the change in streamflow (Figure 8). The mean monthly sediment loads (from 3 RCMs) at the basin outlet is projected to vary between −39% and 128% under RCP 2.6 and between −63% and 217% under RCP 8.5 at mid-century compared with the baseline period. Similarly, simulations project that sediment loads will vary between −19% and 158% (RCP 2.6) and −57% and 922% (RCP 8.5) at the end of the century for RCP 8.5. Under RCP 8.5, the relative changes in the sediment loads also follow the months and RCMs of the highest increase and decrease in streamflow (i.e., June and March, and RegCM4/MPI-ESM-MR). In contrast, under RCP 2.6, the highest increase and decrease in monthly sediment loads appeared in January (158%, simulation forced with RegCM4/NCC-NORESM1-M) at the end of the century and February (39%, simulation forced with RegCM4/MPI-ESM-MR) at mid-century. As with the streamflow projections, simulations forced with RegCM4/MPI-ESM-MR generally projected a decrease in monthly sediment loads during the inter-monsoon 1 (March–April). Overall sediment loads are projected to increase more during the SWM period than in other seasons (Figure 8).

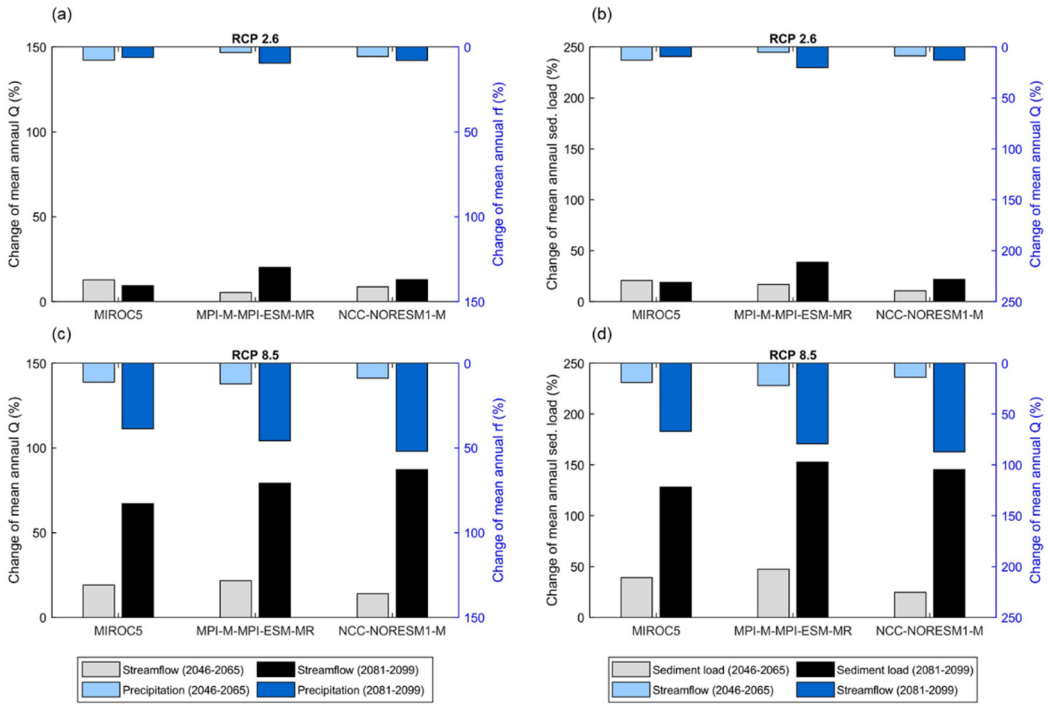

Figure 7. Percentage change in projected mean annual flow (**a**,**c**) and sediment load (**b**,**d**) at basin outlet relative to the baseline period (1991–2005) under RCP 2.6 and RCP 8.5, computed using the three RegCM4 RCM data as forcing. Q is Streamflow and rf is precipitation. Each panel (left and right) shows results for RCP 2.6 (**a**,**b**) and RCP 8.5 (**c**,**d**) and the three RegCM4 RCMs (MIROC5, MPI-M-MPI-ESM-MR, and NCC-NORESM1-M). In each subplot, the light color bar shows results for mid-century (2046–2065), whereas the dark color bar shows results for the end-century (2081–2099). In the left panel, streamflow changes are in the primary axis (left Y-axis), and precipitation changes are in the inverse secondary axis (right Y-axis). Similarly, in the right panel, sediment load changes are in the primary axis, and streamflow changes are in the inverse secondary axis.

The peak months of sediment loads are similar to those of streamflow peaks in all but one case. The only exception is projected with RCP 8.5 inputs of RegCM4/MIROC5 data where the sediment peak occurs in April, while the streamflow peak occurs in June at the end of the century (2081–2099). During 2081–2099, MIROC5 data-driven SWAT simulations show seven (out of 228) high sediment loads (>0.5 million tons/ month) and a high streamflow (>800 m^3/s). Of these sediment peaks, only one is projected to occur in April, with four peaks in May and the remaining two in October. The high sediment loads in April (2 million tons/ month) are projected for 2099, which is the underlying reason the average monthly sediment peak over the 2081–2099 period shifted to April. If 2099 is omitted from the averaging, peaks of both streamflow and sediment loads will occur in May.

Just as climate change affects the annual streamflow variation, it is projected to increase the annual sediment loads of the Kalu RB (Figure 7). The annual sediment loads are projected to increase by 11–21% and 19–39% for RCP 2.6 during mid-and end-century periods, respectively, whereas under RCP 8.5, these increases are 25–48% and 128–153% for the two periods, respectively.

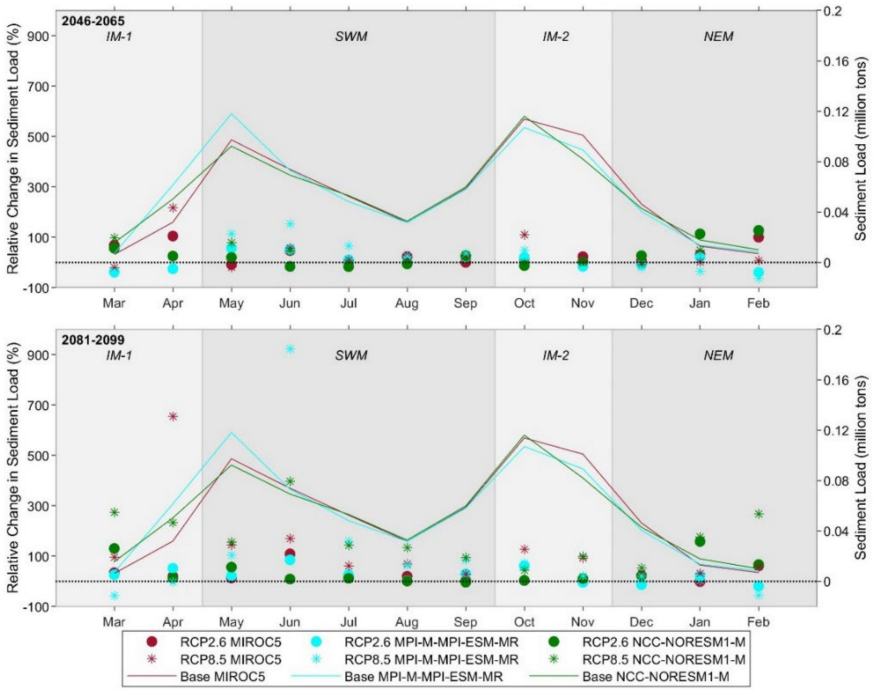

Figure 8. Percentage change in projected mean monthly sediment loads at the basin outlet relative to the baseline period (1991–2005) and absolute sediment loads for simulations of individual RegCM4 RCM. In each panel, relative changes for future periods are in the primary (left Y-axis) and sediment loads for baseline periods are in the secondary axis (right Y-axis). The top panel shows the mid-century period (2046–2065), and the bottom panel shows the end-century period (2081–2099). Each panel shows the results of three RegCM4 RCMs (MIROC5, MPI-M-MPI-ESM-MR, and NCC-NORESM1-M) under RCP 2.6 and 8.5. The shaded areas represent the four monsoon seasons.

In general, an increase or decrease in streamflow corresponds to the sediment loads at monthly, seasonally, and annual time scales. These variations in sediment loads are always higher than the projected changes in streamflow. Similar findings were observed in a study carried out in the Nam Ou Basin (Lao PDR) [30]. In that study, −27 to 160% variation in sediment loads was projected to correspond for −17 to 66% changes in annual streamflow for downscaled five GCMs and three emission scenarios. Similarly, simulations forced with bias-corrected GCM model (BNU-ESM) data show that the average annual runoff in the headwaters of the Yinma RB (China) is projected to increase by 88% and 48% during 2021–2050 for RCP 4.5 and RCP 8.5, respectively, leading to sediment load increases of 237% and 133% for RCP 4.5 and 8.5, respectively [46]. Sirisena et al. (2021) [47] also found similar results for the Irrawaddy RB, Myanmar, in which simulations forced with bias-corrected three GCMs show that under RCP 2.6 and RCP 8.5, streamflow is projected to increase by 8–17% and 9–45%, and sediment loads by 13–26% and 18–75%, respectively, at the end of the century (2081–2100) compared with the baseline period (1991–2005).

4. Conclusions

This study assessed the impact of climate change on future streamflow and sediment loads in the Kalu River Basin, Sri Lanka. The hydrological simulations (using SWAT) were presented for the baseline period (1991–2005) and two future periods: mid-century (2046–2065) and end of the century (2081–2099). Climate data (i.e., precipitation and minimum and maximum temperatures) from three high resolution (25 km) regional climate models (RCMs) were corrected for biases using the mean-bias correction method before forcing the SWAT model.

The hydrological model (forced with observed precipitation and temperature data) was calibrated over the 1991–2000 period, achieving a reasonable agreement with streamflow values at three gauging stations. Further, manual soft calibration was performed

for sediment loads with the limitedly available annual observed sediment loads at the basin outlet, achieving reasonable results. SWAT model simulations forced with the bias-corrected RCM data (i.e., precipitation and maximum and minimum temperatures) projected the streamflow and sediment loads for the baseline period (1991–2005) reasonably well, although with some overestimation.

By the end of the century, the KRB is projected to become warmer and wetter than current climate conditions (1991–2005 as baseline). In general, streamflows and sediment loads are projected to increase during the southwest monsoon (SWM) period compared with other periods of the year (Inter-monsoons (IM-1 and 2) and northeast monsoon (NEM)). The projected percentage changes in sediment loads are higher than those in streamflow. At the end of the century (2081–2099), under RCP 8.5, all simulations project an increase of 67–87% in streamflow and an increase of 128–145% in sediment loads compared with the baseline period across the three RCMs.

As this study is the "first of its kind" climate change-driven impacts on hydrological responses in a basin carried out with finer resolution RCMs under AR5 emission scenarios in the Sri Lanka context, these findings can be a benchmark for future studies for other river basins. Increased precipitation and the resultant streamflow will affect many socio-economic sectors of the Kalu River Basin because of the high risk of flooding in terms of volume and frequency. At the same time, the projected increase in sediment loads to the coast may positively affect the coastal zone (in the absence of sand mining). Due to the ever-increasing demands of a growing population (e.g., food, water, and housing), land-use change in the basin is inevitable. Streamflow and sediment yield is highly dependent on the land-use pattern within the basin. As this study did not consider the effects of land-use changes, further studies that incorporate impacts of land-use change can complement the current study to understand the compounding impacts of climate and land-use changes in the KRB.

Supplementary Materials: The following are available online at https://www.mdpi.com/article/10.3390/w13213031/s1, Figure S1: Gridded average annual precipitation, minimum and maximum temperatures, Figure S2: Average monthly precipitation from three RCMs over the Kalu River Basin, and Table S1: Hydrological parameters used in model calibration.

Author Contributions: Conceptualization, T.A.J.G.S. and S.M.; methodology, T.A.J.G.S., S.M. and R.R.; simulations, T.A.J.G.S.; formal analysis, T.A.J.G.S.; data curation, T.A.J.G.S., E.C. and J.B.; writing—original draft preparation, T.A.J.G.S.; writing—review and editing, S.M., J.B., E.C. and R.R.; supervision, R.R. and S.M. All authors have read and agreed to the published version of the manuscript.

Funding: This study is a part of T.A.J.G.S.'s Ph.D. research, which was supported by the EPP Myanmar project and the Netherlands Fellowship Programme (NFP).

Institutional Review Board Statement: Not applicable.

Informed Consent Statement: Not applicable.

Data Availability Statement: The raw data supporting the conclusions of this article will be made available by the authors, upon request.

Acknowledgments: T.A.J.G.S. was supported by the EPP Myanmar project and Netherlands Fellowship Programme (NFP). RR is supported by the AXA Research Fund.

Conflicts of Interest: The authors declare no conflict of interest.

References

1. Stocker, T.F.; Qin, D.; Plattner, G.-K.; Tignor, M.; Allen, S.K.; Boschung, J.; Nauels, A.; Xia, Y.; Bex, V.; Midgley, P.M. (Eds.) *IPCC Climate Change 2013: The Physical Science Basis. Contribution of Working Group I to the Fifth Assessment Report of the Intergovernmental Panel on Climate Change*; IPCC, Cambridge University Press: Cambridge, UK; New York, NY, USA, 2013.

2. Shukla, P.R.; Skea, J.; Buendia, E.C.; Masson-Delmotte, V.; Pörtner, H.-O.; Roberts, D.C.; Zhai, P.; Slade, R.; Connors, S.; van Diemen, R. (Eds.) IPCC Summary for Policymakers. In *Climate Change and Land: An IPCC Special Report on Climate Change, Desertification, Land Degradation, Sustainable Land Management, Food Security, and Greenhouse Gas Fluxes in Terrestrial Ecosystems*; IPCC: Geneva, Switzerland, 2019.
3. Core Writing Team; Pachauri, R.K.; Meyer, L.A. (Eds.) *IPCC Climate Change 2014: Synthesis Report. Contribution of Working Groups I, II and III to the Fifth Assessment Report of the Intergovernmental Panel on Climate Change*; IPCC: Geneva, Switzerland, 2014; p. 151. ISBN 9789291691432.
4. Eckstein, D.; Dorsch, L.; Fischer, L. *Global Climate Risk Index 2020*; Germanwatch e.V.: Bonn, Germany, 2019; ISBN 9783943704044.
5. Baba, N. Sinking the Pearl of the Indian Ocean: Climate Change in Sri Lanka. *Glob. Major. E-J.* **2010**, *1*, 4–16.
6. World Bank. *Turn Down the Heat: Climate Extremes, Regional Impacts, and the Case for Resilience*; International Bank for Reconstruction and Development/The World Bank: Washington, DC, USA, 2013.
7. De Costa, W.A.J.M. Climate change in Sri Lanka: Myth or reality? Evidence from long-term meteorological data. *J. Natl. Sci. Found. Sri Lanka* **2008**, *36*, 63–88. [CrossRef]
8. Eriyagama, N.; Smakhtin, V. Observed and projected climatic changes, their impacts and adaptation options for Sri Lanka: A review. In Proceedings of the National Conference on Water, Food Security and Climate Change, Colombo, Sri Lanka, 9–11 June 2009; pp. 99–117.
9. Chandrapala, L. Long-term Trends of Rainfall and Temperature in Sri Lanka. In *Climate Variability and Agriculture*; Abrol, Y.P., Gadgil, S., Pant, G.B., Eds.; Narosa Publishing House: New Delhi, India, 1996; pp. 153–162.
10. Ampitiyawatta, A.D.; Guo, S. Precipitation Trends in the Kalu Ganga Basin in Sri. *J. Agric. Sci.* **2009**, *4*, 10–18. [CrossRef]
11. Eriyagama, N.; Smakhtin, V.; Chandrapala, L.; Fernando, K. *Impacts of Climate Change on Water Resources and Agriculture in Sri Lanka: A Review and Preliminary Vulnerability Mapping*; International Water Management Institute: Colombo, Sri Lanka, 2010.
12. Nandalal, K.D.W. Use of a hydrodynamic model to forecast floods of Kalu River in Sri Lanka. *Spec. Issue J. Flood Risk Manag. Integr. Flood Manag.* **2009**, *2*, 151–158. [CrossRef]
13. Chen, J.; Brissette, F.P.; Zhang, X.J.; Chen, H.; Guo, S.; Zhao, Y. Bias correcting climate model multi-member ensembles to assess climate change impacts on hydrology. *Clim. Chang.* **2019**, *153*, 361–377. [CrossRef]
14. Sharma, D.; Das Gupta, A.; Babel, M.S. Spatial disaggregation of bias-corrected GCM precipitation for improved hydrologic simulation: Ping River Basin, Thailand. *Hydrol. Earth Syst. Sci.* **2007**, *11*, 1373–1390. [CrossRef]
15. Smitha, P.S.; Narasimhan, B.; Sudheer, K.P.; Annamalai, H. An improved bias correction method of daily rainfall data using a sliding window technique for climate change impact assessment. *J. Hydrol.* **2018**, *556*, 100–118. [CrossRef]
16. Teutschbein, C.; Seibert, J. Bias correction of regional climate model simulations for hydrological CC-impact studies_Review and evaluation of different methods. *J. Hydrol.* **2012**, *456–457*, 12–29. [CrossRef]
17. Nyunt, C.T.; Yamamoto, H.; Yamamoto, A.; Nemoto, T.; Kitsuregawa, M.; Koike, T. Application of bias-correction and downscaling method to Kalu Ganga Basin in Sri Lanka. *Annu. J. Hydraul. Eng.* **2012**, *56*, 115–120. [CrossRef]
18. Schulz, L.; Kingston, D.G. GCM-related uncertainty in river flow projections at the threshold for "dangerous" climate change: The Kalu Ganga river, Sri Lanka. *Hydrol. Sci. J.* **2017**, *62*, 2369–2380. [CrossRef]
19. Arnold, J.G.; Srinivasan, R.; Muttiah, R.S.; Williams, J.R. Large area hydrologic modeling and assessment Part I: Model development. *JAWRA J. Am. Water Resour. Assoc.* **1998**, *34*, 73–89. [CrossRef]
20. Neitsch, S.L.; Arnold, J.G.; Kiniry, J.R.; Williams, J.R. *Soil & Water Assessment Tool Theoretical Documentation Version 2009*; Texas Water Resources Institute: College Station, TX, USA, 2011.
21. Jarvis, A.; Nelson, A.; Guevara, E.; Jarvis, A.; Reuter, H.I.; Nelson, A.; Guevara, E. Hole-Filled SRTM for the Globe Version 4. 2008. Available online: http://srtm.csi.cgiar.org (accessed on 1 August 2016).
22. FAO. *The Digital Soil Map of the World (Version 3.6)*; FAO/UNESCO: Rome, Italy, 2003.
23. Maskey, S. *HyKit: A Tool for Grid-Based Interpolation of Hydrological Variables, User's Guide (Version 1.3)*; IHE Delft Institute for Water Education: Delft, The Netherlands, 2013; pp. 1–6.
24. Arnold, J.G.; Kiniry, J.R.; Srinivasan, R.; Williams, J.R.; Haney, E.B.; Neitsch, S.L. Soil & Water Assessment Tool: Input/output documentation. Version 2012. *Texas Water Resour. Inst.* **2012**, *TR-439*, 650.
25. Abbaspour, K.C. *SWAT-Calibration and Uncertainty Programs (CUP)*; Eawag—Swiss Federal Institute of Aquatic Science and Technology: Duebendorf, Switzerland, 2015. ISBN 9780975840047.
26. Sirisena, T.A.J.G.; Maskey, S.; Ranasinghe, R.; Babel, S. Effects of different precipitation inputs on streamflow simulation in the Irrawaddy River Basin, Myanmar. *J. Hydrol. Reg. Stud.* **2018**, *19*, 265–278. [CrossRef]
27. Masih, I.; Maskey, S.; Uhlenbrook, S.; Smakhtin, V. Assessing the impact of areal precipitation input on streamflow simulations using the SWAT model. *J. Am. Water Resour. Assoc.* **2011**, *47*, 179–195. [CrossRef]
28. Abbaspour, K.C.; Yang, J.; Maximov, I.; Siber, R.; Bogner, K.; Mieleitner, J.; Zobrist, J.; Srinivasan, R. Modelling hydrology and water quality in the pre-alpine/alpine Thur watershed using SWAT. *J. Hydrol.* **2007**, *333*, 413–430. [CrossRef]
29. Sirisena, T.A.J.G.; Maskey, S.; Ranasinghe, R. Hydrological Model Calibration with Streamflow and Remote Sensing Based Evapotranspiration Data in a Data Poor Basin. *Remote Sens.* **2020**, *12*, 3768. [CrossRef]
30. Shrestha, B.; Babel, M.S.; Maskey, S.; Van Griensven, A.; Uhlenbrook, S.; Green, A.; Akkharath, I. Impact of climate change on sediment yield in the Mekong River basin: A case study of the Nam Ou basin, Lao PDR. *Hydrol. Earth Syst. Sci.* **2013**, *17*, 1–20. [CrossRef]

31. Abbaspour, K.C.; Rouholahnejad, E.; Vaghefi, S.; Srinivasan, R.; Yang, H.; Kløve, B. A continental-scale hydrology and water quality model for Europe: Calibration and uncertainty of a high-resolution large-scale SWAT model. *J. Hydrol.* **2015**, *524*, 733–752. [CrossRef]
32. Legates, D.R.; McCabe, G.J., Jr. Evaluating the use of "Goodness of Fit" measures in hydrologic and hydroclimatic model validation. *Water Resour. Res.* **1999**, *35*, 233–241. [CrossRef]
33. Pushpalatha, R.; Perrin, C.; Moine, N.L.; Andréassian, V. A review of efficiency criteria suitable for evaluating low-flow simulations. *J. Hydrol.* **2012**, *420–421*, 171–182. [CrossRef]
34. CCD. *Gazette Extraordinary of the Democratic Socialist Republic of Sri Lanka 2006*; Coast Conservation Department: Colombo, Sri Lanka, 2006; pp. 1–58.
35. Moriasi, D.N.; Arnold, J.G.; Van Liew, M.W.; Binger, R.L.; Harmel, R.D.; Veith, T.L. Model evaluation guidelines for systematic quantification of accuracy in watershed simulations. *Am. Soc. Agric. Biol. Eng.* **2007**, *50*, 885–900. [CrossRef]
36. Giorgi, F.; Coppola, E.; Solmon, F.; Mariotti, L.; Sylla, M.B.; Bi, X.; Elguindi, N.; Diro, G.T.; Nair, V.; Giuliani, G.; et al. RegCM4: Model description and preliminary tests over multiple CORDEX domains. *Clim. Res.* **2012**, *52*, 7–29. [CrossRef]
37. Teichmann, C.; Jacob, D.; Remedio, A.R.; Remke, T.; Buntemeyer, L.; Hoffmann, P.; Kriegsmann, A.; Lierhammer, L.; Bülow, K.; Weber, T.; et al. Assessing mean climate change signals in the global CORDEX-CORE ensemble. *Clim. Dyn.* **2021**, *57*, 1269–1292. [CrossRef]
38. Wang, L.; Ranasinghe, R.; Maskey, S.; van Gelder, P.H.A.J.M.; Vrijling, J.K. Comparison of empirical statistical methods for downscaling daily climate projections from CMIP5 GCMs: A case study of the Huai River Basin, China. *Int. J. Climatol.* **2016**, *36*, 145–164. [CrossRef]
39. Lenderink, G.; Buishand, A.; Van Deursen, W. Estimates of future discharges of the river Rhine using two scenario methodologies: Direct versus delta approach. *Hydrol. Earth Syst. Sci.* **2007**, *11*, 1145–1159. [CrossRef]
40. Schmidli, J.; Frei, C.; Vidale, P.L. Downscaling from GCM precipitation: A benchmark for dynamical and statistical downscaling methods. *Int. J. Climatol.* **2006**, *26*, 679–689. [CrossRef]
41. Hewawasam, T. Effect of land use in the upper Mahaweli catchment area on erosion, landslides and siltation in hydropower reservoirs of Sri Lanka. *J. Natn. Sci. Found. Sri Lanka* **2010**, *38*, 3–14. [CrossRef]
42. Dissanayake, C.B.; Rupasinghe, M.S. Environmental impact of mining, erosion and sedimentation in Sri Lanka. *Int. J. Environ. Stud.* **1996**, *51*, 35–50. [CrossRef]
43. Ahmed, M.; Suphachalasai, S. *Assessing the Costs of Climate Change and Adaptation in South Asia*; Asian Development Bank: Manila, Philippines, 2014.
44. Imbulana, N.; Gunawardana, S.; Shrestha, S.; Datta, A. Projections of extreme precipitation events under climate change scenarios in Mahaweli River Basin of Sri Lanka. *Curr. Sci.* **2018**, *114*, 1495–1509. [CrossRef]
45. Zheng, H.; Chiew, F.H.S.; Charles, S.; Podger, G. Future climate and runoff projections across South Asia from CMIP5 global climate models and hydrological modelling. *J. Hydrol. Reg. Stud.* **2018**, *18*, 92–109. [CrossRef]
46. Zhou, Y.; Xu, Y.J.; Xiao, W.; Wang, J.; Huang, Y.; Yang, H. Climate Change Impacts on Flow and Suspended Sediment Yield in Headwaters of High-Latitude Regions—A Case Study in China's Far Northeast. *Water* **2017**, *9*, 966. [CrossRef]
47. Sirisena, T.A.J.G.; Maskey, S.; Bamunawala, J.; Ranasinghe, R. Climate change and reservoir impacts on 21st-century streamflow and fluvial sediment loads in the Irrawaddy River, Myanmar. *Front. Earth Sci. Hydrosph.* **2021**, *9*, 1–16. [CrossRef]